

#### ARTICLE INFO:

Received : May 15, 2018

Revised : August 21, 2018

Accepted : October 10, 2018

CT&F - Ciencia, Tecnología y Futuro Vol 9, Num 1 June 2019. pages 15 - 26

DOI : <https://doi.org/10.29047/01225383.148>



# QUANTITATIVE EVALUATION OF THE DIAGENESIS AND POROSITY EVOLUTION OF TIGHT SANDSTONE RESERVOIRS: A CASE STUDY OF THE YANCHANG FORMATION IN THE SOUTHERN ORDOS BASIN, CHINA

■ EVALUACIÓN CUANTITATIVA DE LA DIAGÉNESIS Y DE LA EVOLUCIÓN DE LA POROSIDAD DE YACIMIENTOS DE ARENAS COMPACTAS: UN CASO DE ESTUDIO DE LA FORMACIÓN YANCHANG EN LA CUENCA ORDOS DEL SUR, CHINA.

Meng, Xiao<sup>a\*</sup>; Guiqiang, Qiu<sup>c</sup>; Xuanjun, Yuan<sup>a</sup>; Songtao, Wu<sup>ab</sup>; Dawei, Cheng<sup>a</sup>; Chunfang, Chen<sup>c</sup>

## ABSTRACT

Evaluation of the pore evolution is key to gaining a better understanding of oil migration and accumulation in tight oil exploration for tight sandstone; to study the diagenesis and porosity evolution of tight sandstone reservoirs, we analysed the 8<sup>th</sup> member of the Yanchang Formation by core observation, thin section observation, cathodoluminescence, scanning electron microscopy, and logging data analysis. The following conclusions can be drawn (1) In the typical tight sandstone reservoir, numerous secondary pores developed at burial depths in the range of 1300 m to 1400 m, and approximately 1500 m to 1600 m. (2) Compaction was the most influential factor of reservoir density and decreased the average pore size by 24.8%. Carbonate cementation decreased the porosity by 8.2%. The most important diagenetic process for increasing the reservoir porosity was dissolution, which increased the pore size by 5.1%. In addition, chlorite played an active role in inhibiting secondary quartz growth and preserving primary pores. (3) The early gas invasion can inhibit diagenesis, and the organic acids produced by the later oil can increase dissolution, so that the high oil saturation phenomenon becomes more obvious.

## RESUMEN

La evaluación de la evolución de los poros es clave para obtener una mejor comprensión de la migración y acumulación de petróleo en la exploración de petróleo para arenas compactas; Para estudiar la diagénesis y la evolución de la porosidad de los reservorios de arenas compactas, se analizó el octavo componente de la Formación Yanchang a través de la observación de núcleos, la observación de secciones delgadas, análisis de catodoluminiscencia, microscopía electrónica de barrido y análisis de registro de datos.

Del presente estudio se pueden extraer las siguientes conclusiones (1) En los reservorios característicos de arenas compactas, se desarrollaron numerosos poros secundarios a profundidades de enterramiento en el rango de 1300 a 1400 m, y de aproximadamente

1500 m a 1600 m. (2) La compactación fue el factor más influyente en la densidad del yacimiento y disminuyó el tamaño promedio de los poros en un 24.8%. La cementación por carbonato disminuyó la porosidad en un 8,2%. Mientras que el proceso diagenético más importante para aumentar la porosidad del yacimiento fue la disolución, que aumentó el tamaño de los poros en un 5,1%.

Además, la clorita desempeñó un papel activo en la inhibición del crecimiento secundario del cuarzo y en la conservación de los poros primarios. (3) La invasión temprana de gas puede inhibir la diagénesis, y los ácidos orgánicos producidos posteriormente por el petróleo pueden aumentar la disolución, por lo que el fenómeno de alta saturación de petróleo se hace más significativo.

## KEYWORDS / PALABRAS CLAVE

Reservoir Characteristics | Diagenesis  
Pore Evolution | Ordos Basin.  
Características del reservorio | Diagénesis |  
Evolución de poros | Cuenca Ordos

## AFFILIATION

<sup>a</sup> PetroChina Research Institute of Petroleum Exploration and Development, Beijing 100083, China.

<sup>b</sup> State Key Laboratory of Enhance Oil Recovery, Beijing 100083, China.

<sup>c</sup> SINOPEC Exploration Production Researcher Institute, Beijing 100083, China.

\*email: xiaomeng422@126.com

## 1 INTRODUCTION

Unconventional oil plays with considerable resources are receiving increasing attention [1]-[5]. At the end of 2010, the total proven remaining oil reserves in the global conventional petroleum plays amounted to 1888×108t, accounting for 40% of the global oil and gas reserves [6]. The primary development of future resources will shift from conventional to unconventional. Currently, tight oil has achieved a breakthrough in the Bakken (Williston Basin, North America) [7]-[8] and the Eagle Ford formations [9]. According to a 2012 prediction from the International Energy Agency (IEA), the remaining global recoverable resources of tight oil are 327×108 t, which is exploitable with the proper technology [10]. Besides shale gas, tight oil is considered the most practical unconventional successor for conventional oil and gas [11]-[12].

Tight sandstone is a reservoir which porosity is less than 10% and air permeability less than 1mD [13]. Tight sandstone reservoirs have undergone complex diagenetic evolution and structural changes [14]. The pore structure of tight sandstone reservoirs with small pore throat diameter, poor connectivity and strong heterogeneity is different from that of conventional sandstone reservoirs. [15]-[17] The pore system of tight reservoirs is mainly micron - nanometer pore throat system, and the nanometer orifice throat is dominant [18]. Quantitative diagenesis evaluation of sandstone reservoirs is still debated [19]. A tight sandstone reservoir is strongly

heterogeneous and difficult to explore and develop [20]-[21]. The development of effective reservoirs has an important influence on tight oil and gas production. Therefore, the quantitative evaluation of the diagenesis in tight sandstone reservoirs is important for oil exploration [22].

The Yanchang Formation in the southern Ordos Basin has rich resources [23]-[24]. The reservoir in Chang 8<sup>th</sup> member is a typical tight sandstone reservoir, in which oil and gas are mainly concentrated in the micro-cracks and reservoir sweet spots [25]. Researchers who studied these reservoir sweet spots in the past [26]-[27] believe that early sedimentation determines the type and intensity of diagenesis and that late diagenesis primarily drives reservoir densification [28].

The Binchang area in the southern Ordos Basin is a Sinopec exploration area; It is expected that by the end of 2011 the Chang 8<sup>th</sup> member reserves will be 95.72 million, and its forecast reserves will be 34.63 million t. Numerous wells have produced oil economically, and good prospects have been identified in the study area. Current exploration and research activity in the Binchang area is low; therefore, an in-depth study of the diagenesis characteristics and evolution in the Chang 8<sup>th</sup> member is required to predict promptly the occurrence of effective and high-quality reservoirs.

## 2. THEORETICAL FRAME

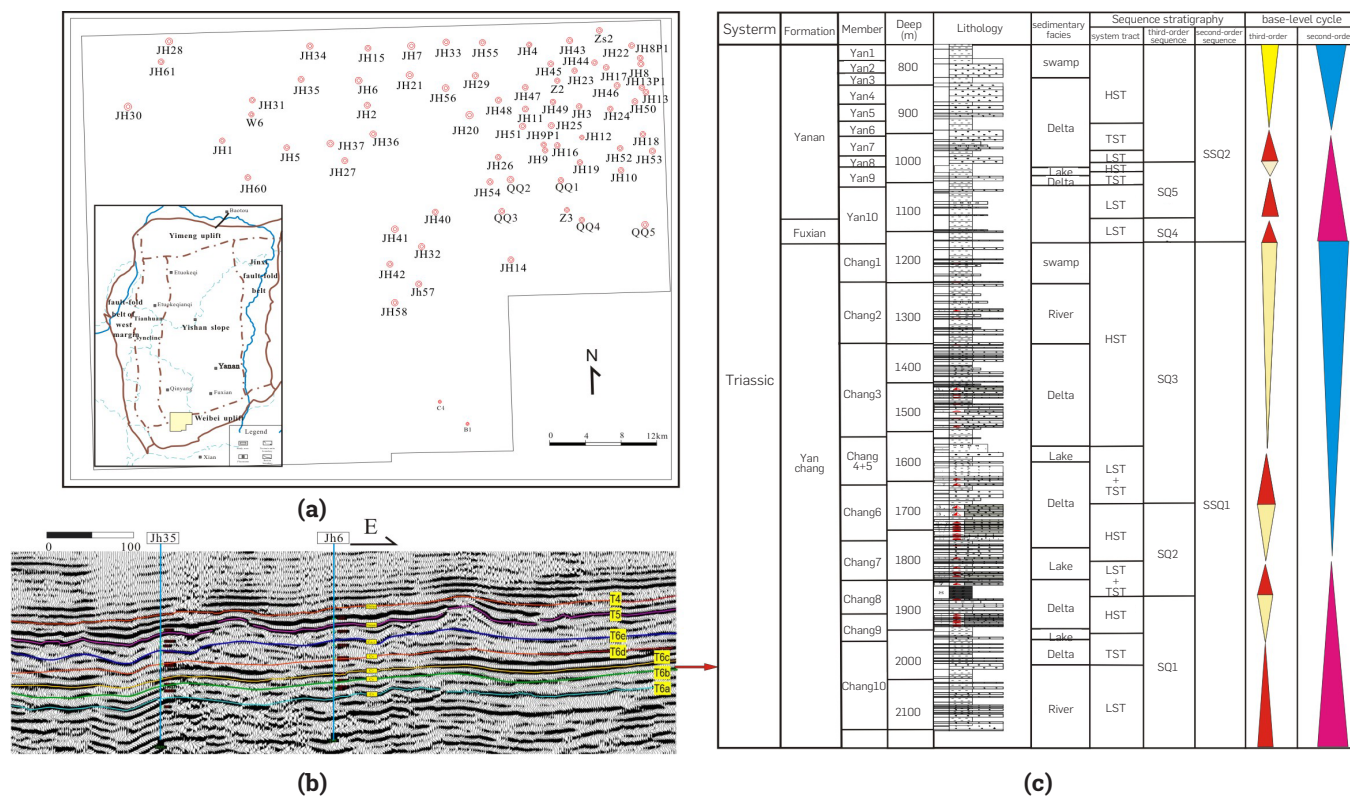


**Figure 1.** (a) Location map of the Binchang area in the Ordos Basin. (b) Seismic profiles in the studied area (c) The generalized stratigraphy of the Binchang region in the Ordos Basin.

The Yanchang Formation mainly developed as a delta sedimentary system within a continental basin; the basin can be divided into six first-order tectonic units [29]-[30] the Tianhuan syncline, the fault-fold belt at the western margin, the Yimeng uplift, the Yishan slope, the Jinxi fault-fold belt and the Weibei uplift (**Figure 1**). This lacustrine basin is elongated in the north-south direction, and it is shallower and steeper in the northern area. The main sediment source during the early period of deposition was to the southwest of the basin. In the middle and late periods of deposition, the main sediment sources were to the northeast [31]-[32]. Binchang is located at the structural junction of the Yishan slope and the Weibei uplift (**Figure 1a**). The study area is not structurally developed, but a small anticline has formed in the western study area [33]-[34].

The burial depth of the interior of the basin reached its maximum during the Yanshan movement in the Late Cretaceous (**Figure 1b**), when most of the Yanchang Formation was below 2100 m. Subsequently, oil and gas began extensive migration and accumulation [35]-[36]. In the late stage of migration and accumulation, the entire basin was uplifting to the southeast, and this tectonic tilt continues to date [37]-[38].

The Yanchang Formation, in the southern Ordos Basin, is divided into one first-order sequence (the Yanchang Formation), two second-order sequences (Chang 10 to Chang 7 and Chang 6 to Chang 1), and four third-order sequences (Chang 10 and Chang 9, Chang 8 and Chang 7, Chang 6 to Chang 4+5, and Chang 3 to Chang 1) [38]-[39] (**Figure 1c**).

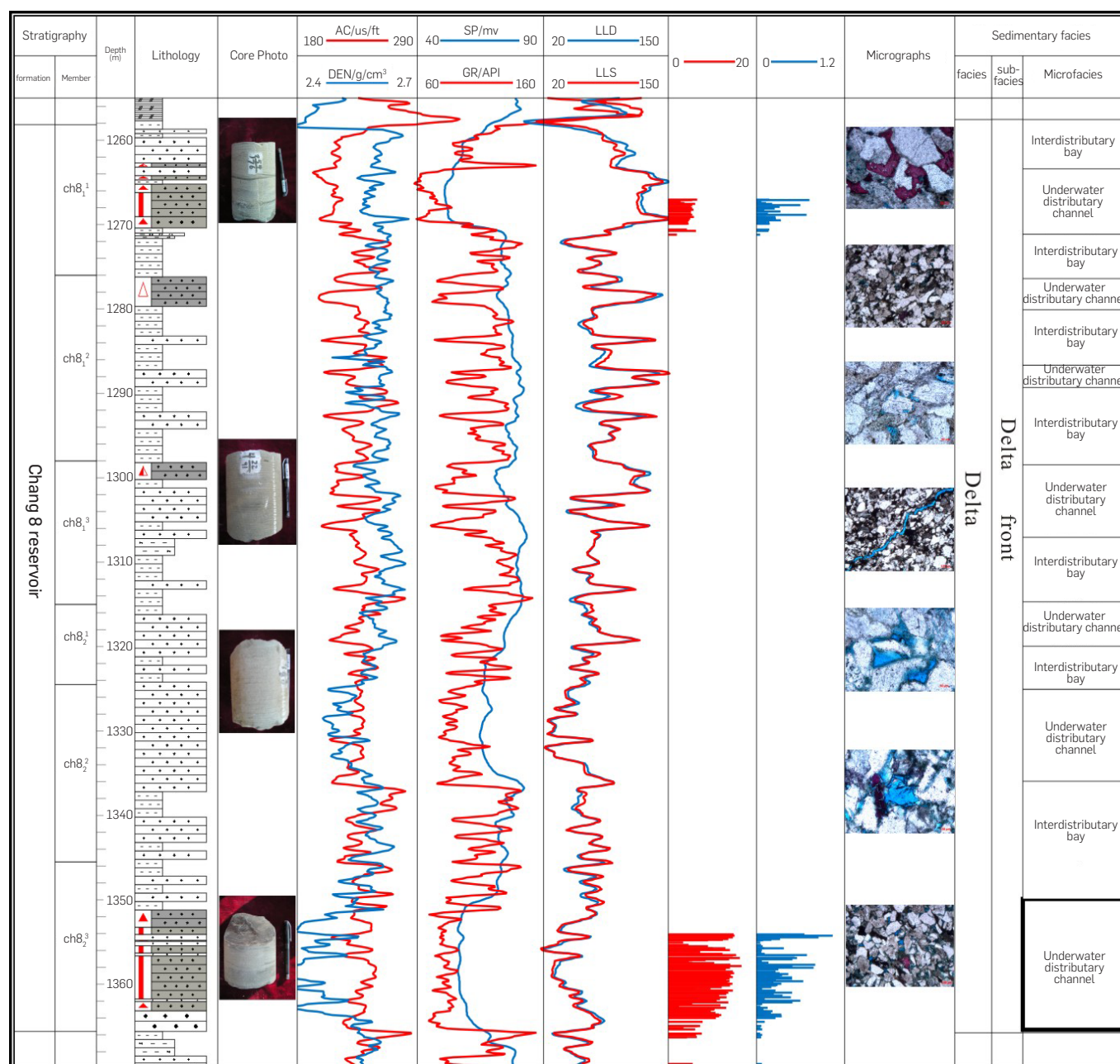


**Figure 2.** The well profile of the JH8 in the Binchang area.

Previous studies indicated that sedimentary facies control the original physical properties of the reservoir at a microscopic scale of Yanchang Formation [40]. Chang 8<sup>th</sup> is the main oil-bearing layer in the Binchang area. According to the oil and gas show and test data (from Huabei Petroleum Bureau, Sinopec), the northeast study area is the main oil-producing area. The date of source rock correlation shows that the seventh member of the Yanchang Formation, just under the Chang 8<sup>th</sup> member, is the main source rock of Chang 8<sup>th</sup> reservoirs [41]. The Chang 8<sup>th</sup> reservoir of the Yanchang Formation is dominated by delta-front sedimentation, where a subaqueous distributary channel and distributary channel bay are developed. The underwater distributary channel (Figure 2) frames the reservoir and is the most favourable reservoir development zone.

### 3. EXPERIMENTAL DEVELOPMENT

In the study, numerous drillings for oil have taken place in this area. There is plenty of exploration and production well data to support this paper, mainly derived from 43 wells.

400 rock composition data, 400 grading data, 2386 porosity and permeability data, 200 mercury injection capillary pressure testing data and well logging data sets for 137 wells were obtained from the research Institute of HuaBei Oilfield Company, Sinopec.

Samples of different lithology and sedimentary microfacies were selected from the Chang 8<sup>th</sup> member cores of 43 wells. For the lithology analysis, diagenesis and pore characteristics, 200 polished thin sections and 400 blue or red epoxy resin-impregnated thin sections were grinded. Thin sections were coloured by Alizarin RedS and K-ferricyanide for calcium carbonate cementation identification. Furthermore, 122 fluorescent thin section were used for carbonate mineral identification. Point counting was carried out on 45 thin sections to quantitatively analyze rock composition data, all types of pores and carbonate cements. 44 representative samples were observed by scanning electron microscope (SEM), which was equipped with an energy dispersive X-ray spectrometer. The cathodoluminescence experiment of 122 samples was performed, using an Olympus microscope equipped with a CL8200-MKS CL instrument. In addition, 3-D seismic data from the study area was interpreted, and well log and drilling data from 137 wells was statistically analyzed. Point counting, fluorescent thin section, and scanning electron microscope observations were carried out in the Key laboratory of SINOPEC Exploration Production Researcher Institute.

### 4. RESULTS

#### LITHOLOGY

The lithology analysis of the Chang 8<sup>th</sup> reservoir shows that the lithologic components include 21%-62% quartz (average 36.15%); 15%-47% feldspars (average 30.83%), which are mostly in the K-feldspar (20.8%) and plagioclase (7.1%); and 16%-56% rock fragments (average 33.02%), which are mostly volcanic rock (17.03%) and metamorphic debris (6.7%). According to the Folk classification, the Chang 8<sup>th</sup> sandstones are mostly feldspathic litharenites and lithic arkosic sandstones (Figure 3a), indicating that this region has a lower sandstone compositional maturity.

The sorting degree is moderate (Figure 3b), where fine-grained sandstone is dominant (Figure 3c), and the high content of feldspar and dissolvable lithic material provides the material basis for the formation of dissolution pores.

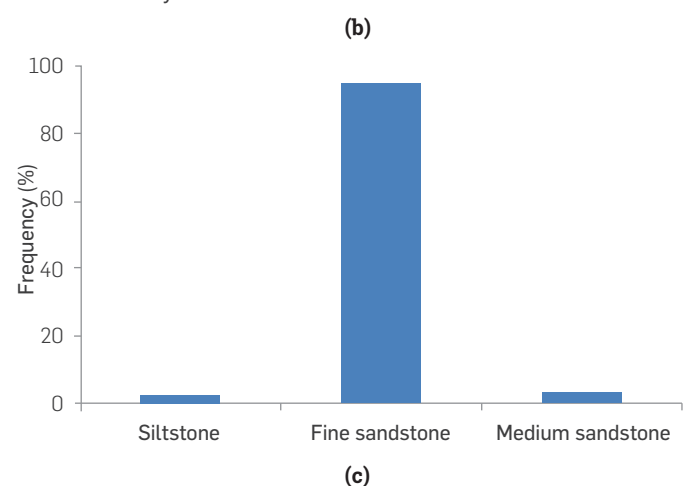
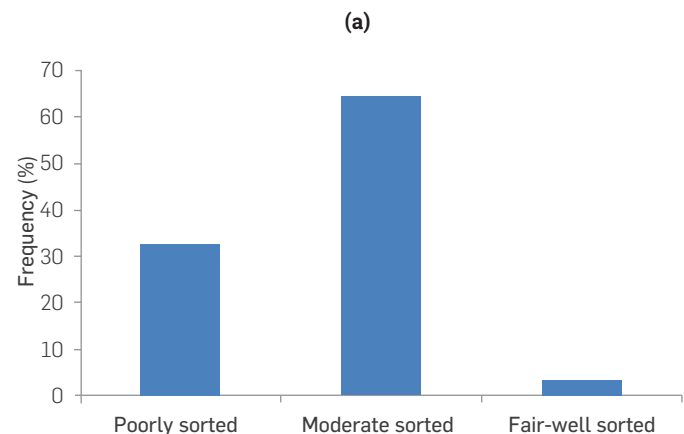
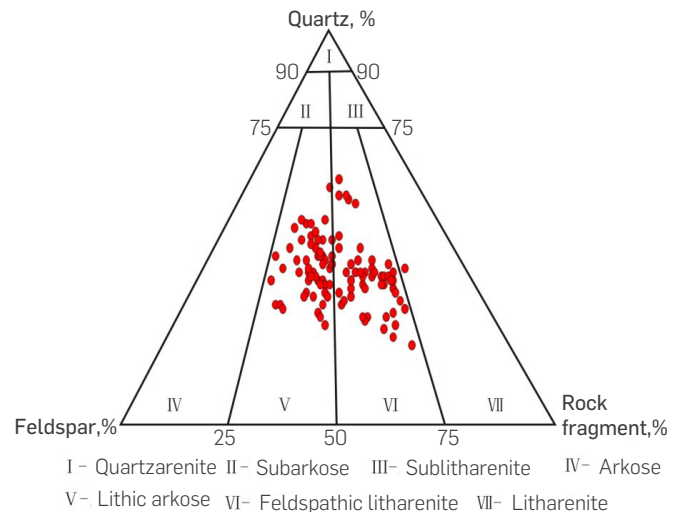


**Figure 3.** Detrital rock composition, lithology and sorting distribution of the Chang 8<sup>th</sup> member in the Binchang region. (a) Folk (1974) classification of the sandstone; (b) Sorting distribution; and (c) Lithology distribution.



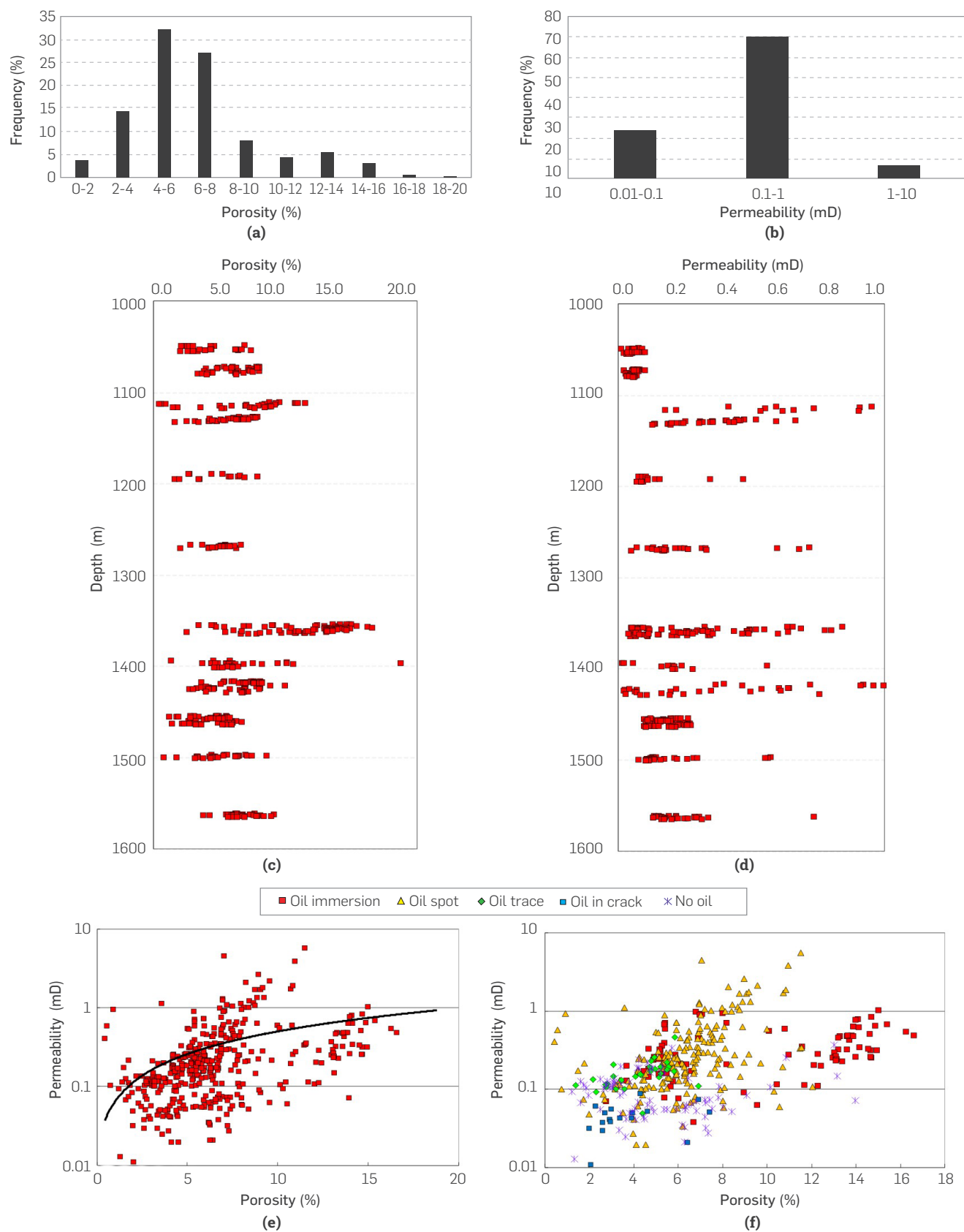


**Figure 4.** The Chang 8<sup>th</sup> tight sandstone reservoir properties characteristics.

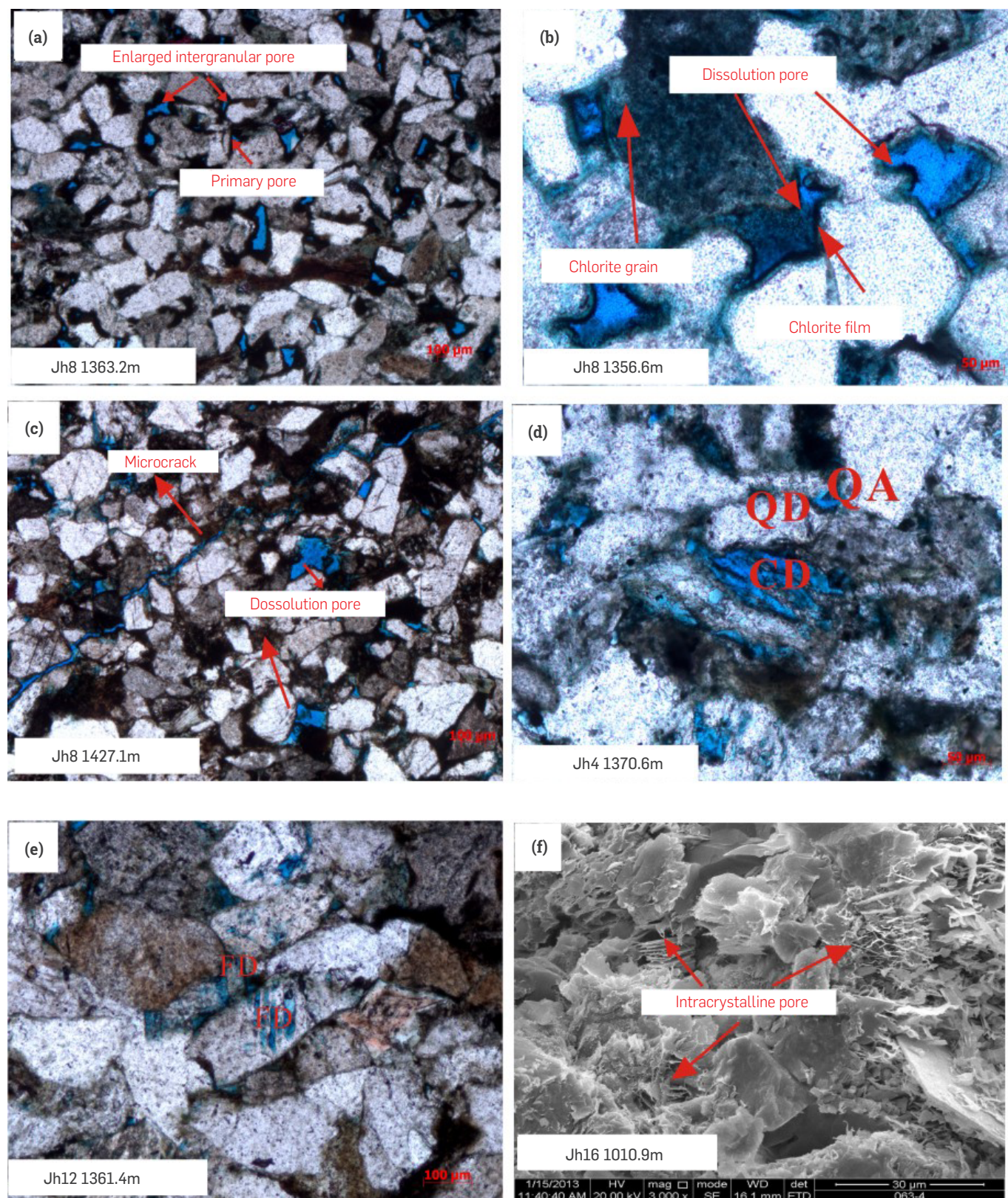


**Figure 5.** The main pore type in the Chang 8<sup>th</sup> member of the Binchang area.



## RESERVOIR PROPERTIES

### POROSITY AND PERMEABILITY

The porosity (measured from 406 thin sections) and the permeability (measured from 405 thin sections) data show that the porosity ranges from 1.2% to 19.8% (average is 6.4%) (**Figure 4a**) and the permeability ranges from 0.013 mD to 9.757 mD (average is 0.362 mD) (**Figure 4b**). The Chang 8<sup>th</sup> member is a low-porosity and low-permeability reservoir.

Based on the comprehensive analysis of the log, core and test data, the relationship between the porosity and the burial depth of the well (**Figure 4c**) and the relation between the permeability and the buried depth (**Figure 4d**) are established. Approximately between 0 m and 1000 m, the porosity rapidly decreases from 35% to 15% due to compaction, and the pore type is mainly intergranular. Between 1000 m and 1100 m, the porosity decreases slowly to approximately 10%, as the depth increases due to mechanical compaction, cementation and dissolution. The primary pore type is intergranular, followed by a smaller number of secondary and intergranular pores. Between 1300 m and 1400 m, the porosity slightly increases with depth, which is related to the formation of secondary pores from the transformation of montmorillonite to illite or chlorite. The pore types are intergranular and secondary dissolution. Between 1400 m and 1500 m, the porosity gradually decreases with increasing depth due to the cementation of calcite. Between 1500 m and 1600 m, the porosity increases with depth due to the source rocks discharging organic acids that dissolve the cementation and clastic particles, forming the secondary pores; microscopically, the dissolved pores are filled by asphalt, indicating that the timing of the secondary pore development is concurrent with the oil accumulation and migration. Below 1600 m, as the burial depth increases, the cementation and pressure dissolution gradually increase, and the porosity gradually decreases. From the above analysis, secondary pores developed between 1300 m and 1400 m and between 1500 m and 1600 m. In addition, porosity and permeability have a good correlation (**Figure 4e**). Further, the better the physical properties, the better the oil content (**Figure 4f**).

### PORE TYPES AND CHARACTERISTICS

Thin section and scanning electron microscopy observations (from 400 thin sections and 200 images) show the pores types in the Chang 8<sup>th</sup> reservoir: primary pores (**Figure 5a**), secondary solution pores (**Figures. 5b,c,e**), and micro-fissures (**Figure 5c**). The dissolution pores and the remaining inter-granular pores primarily create porosity. The primary pores are those remaining after compaction and cementation, and the primary pore edges are flat and triangular; these pores occupy 14% of the plane porosity. The dissolution pores include intra-granular dissolved pores and inter-granular dissolved pores. Inter-granular dissolved pores create the primary reservoir space in the Chang 8<sup>th</sup> reservoir, and the dissolution pore edges are irregular; intergranular dissolved pores occupy 75% of the plane porosity. Microcracks include shrinkage joints and mica cleavage joints, playing a minor role in controlling reservoir properties. The primary pores are generally well connected; however, because of continued compaction and cementation, the reservoir is becoming denser and smaller. The late widespread carbonate cementation further densified the Chang 8<sup>th</sup> member (**Figure 5b**). The secondary pores related to the dissolution of feldspar (**Figure 5e**) and other lithics (**Figure 5d**) and the micro-fractures (**Figure 5c**) considerably increase the quality of the reservoir [42]; furthermore, the inter-crystalline pores within clay minerals contribute to porosity (**Figure 5f**).

in **Figure 5**: (a) Thin-section micrograph showing a primary pore and enlarged intergranular pore; (b) thin-section micrograph showing a dissolution pore; (c) thin-section micrograph showing a micro-fracture; (d) thin-section micrograph showing partly dissolved cuttings; (e) thin-section micrograph showing a completely and partly dissolved feldspar; (f) SEM micrograph showing an intra-crystalline pore.

The statistical analysis results indicate that the average pore-throat radius of the Chang 8<sup>th</sup> reservoir is 0.032  $\mu\text{m}$ ; The smallest pore-throat is the limiting factor of the reservoir properties [43]-[45]. The mercury injection capillary pressure data show that the pore-throat radii range from 0.18  $\mu\text{m}$  to 0.89  $\mu\text{m}$  with an average of 0.316  $\mu\text{m}$ ; the displacement pressures are high and range from 0.41 MPa to 43.19 MPa with an average of 5.86 MPa; and the median pressures are high and range from 1.72 MPa to 171.35 MPa with an average of 33.48 MPa. Reservoir pore and pore-throat sizes are small and unfavourable for fluid migration and accumulation, and the percolation is poor.

### DIAGENETIC CHARACTERISTICS

The Chang 8<sup>th</sup> tight member has undergone multi-stage superimposed modification, including compaction, authigenic quartz, carbonate cementation and clay mineral, leading to reservoir porosity decrease, but dissolution, oil invasion and chlorite film generation led to reservoir porosity increase.

### COMPACTION

The Chang 8<sup>th</sup> reservoir in the Binchang area underwent a medium-intensity compaction, which is the most important factor of reservoir densification. Most of the particle boundaries are in-line contacts and concavo-convex contacts (**Figure 6a**). Under mechanical compaction, the mica deformed and squeezed between particles.

### QUARTZ CEMENTATION

The syntaxial overgrowth and pore-filling cement are the main types of authigenic quartz developed in the study area (**Figure 6c**). Authigenic quartz is related to the formation of kaolinite and subsequent release of  $\text{SiO}_2$  by the k-feldspar, plagioclase, tuffaceous detritus and granite debris dissolution in the acidic environment [46]-[47]. Authigenic quartz occupies pore space, which decreases the reservoir quality [48]. In the early diagenetic period, syntaxial overgrowth generally grew along the edge of quartz particles, and the authigenic quartz more commonly grew between detrital grains (**Figure 6e**). In addition, authigenic quartz is always accompanied by the formation of kaolinite, mixed-layer illite/smectite, and chlorite (**Figures 6f, 6g**). The influence of authigenic quartz on the pore evolution can be neglected, as there is only a small authigenic quartz content in the Chang 8<sup>th</sup>; therefore, the authigenic quartz is not quantitatively discussed in here.

### CARBONATE CEMENTATION

In the Yanchang Formation reservoir of the southern Ordos Basin, which underwent multiple stages of structural subsidence and variations in its fluid properties, carbonate cementation is common in the Chang 8<sup>th</sup> member, carbonate cementation primarily occurred from the late settlement of the basin to the early stage of uplift. The carbonate cementation, which fills part of the inter-granular pores and intra-granular dissolution pores, has a significant destructive effect on the reservoir [49] (**Figure 6b**). The relationship between intergranular volume and cement volume shows that mechanical compaction has played a more important effect in destroying the reservoir porosity of the Chang 8<sup>th</sup> member than cementation (**Figure 7**).

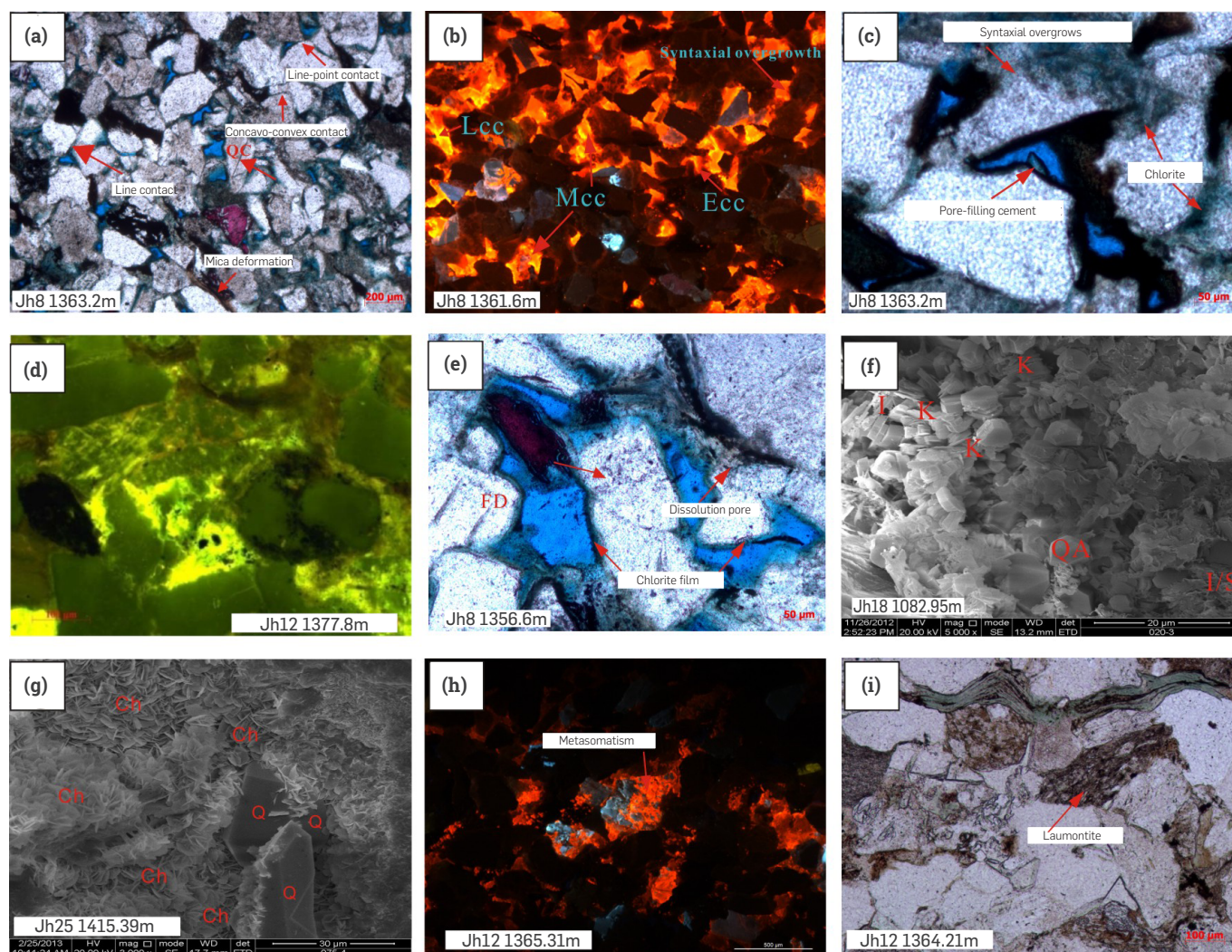


**Figure 6.** Digenesis in the Chang 8<sup>th</sup> member of the Binchang area.

### THE EARLY STAGE OF CHLORITE FILM PRECIPITATION

The authigenic chlorite is observed as a thin-film chlorite structure and a thick pore-lining structure (Figure 6e); the content of chlorite in the Chang 8<sup>th</sup> reservoir ranges between 1.3% and 8%. The first stage of chlorite film formed in the early diagenetic stage A. The chlorite film can inhibit quartz overgrowth and pressure dissolution, increase intergranular compaction strength, and occupy the growth space of carbonate cement [32],[50]–[52]. The chlorite film has a positive effect on reservoir properties. However, as the temperature continued to increase, the mudstone and shale continuously released iron and magnesium, initiating the second stage of chlorite precipitation (Figure 6e) in the pores [53]; consequently, the porosity decreased, and the pore throats narrowed, which had a negative effect on the reservoir properties.

### KAOLINITE PRECIPITATION

The authigenic kaolinite in the study, whose content is approximately 2%, occurs mainly as booklets of vermicularly stacked pseudohexagonal crystals. This kaolinite retains large inter-granular pores and is often associated with authigenic quartz (Figures 6f). The formation of authigenic kaolinite is primarily related to feldspar dissolution and other silicate minerals [42]. If the system is open, the

dissolution ions are removed, and the kaolinite remains in the pores; the intra-crystalline kaolinite pores provide crucial reservoir space in tight sandstone [54]–[57]. The kaolinite precipitation occurred after the feldspar dissolution. Moreover, the kaolinite distribution is strongly heterogeneous and was determined by the heterogeneity of the feldspar dissolution and fluid flow.

### OIL INVASION

Oil invasion plays a positive role in the evolution of the physical properties of reservoirs [58], mainly attributable to the promotion of acid dissolution, inhibition of late carbonate cementation, and weakening of a second stage of quartz growth; these effects strengthen with oil saturation [28],[48],[59]–[61].

From the inclusion testing data, four periods of oil and gas invasion are identified in the Yanchang Formation: The Late Jurassic (154 Ma to 149 Ma), the Early Cretaceous (143 Ma to 107 Ma), the middle Cretaceous (110 Ma to 30 Ma), and the early Tertiary to the late Tertiary (25 Ma to 23 Ma) (Figure 12). The analysis of 200 fluorescent thin sections shows that the migration channels and storage spaces of the early oil invasion are also the main areas for later oil and gas intrusion. The early phase of invasion filled the pore



throats with dark-brown heavy oil, the second phase of yellow oil filled the pores, and the third phase of yellow-green light oil filled the micro-cracks and granular dissolution pores. In the multiple periods of oil invasion, the reservoir properties continued to improve, and the reservoir heterogeneity also increased. A positive correlation is observed between the porosity of the reservoir and the oil saturation. Additionally, the logging results improve as the physical properties of the reservoir improve. In reservoirs with low oil saturations, the oil invasion cannot effectively inhibit the quartz overgrowth and carbonate cementation [62].

## DISSOLUTION

Dissolution is an important diagenetic mechanism of increasing the physical properties of a reservoir. On the one hand, the selective dissolution of particles forms intra-granular pores; on the other hand, dissolution enlarges the inter-granular pores, and the reservoir space increases [63]. According to the chemical properties of a dissolution medium, dissolution can be divided into 2 categories: acid dissolution and alkaline dissolution [59]. Feldspar dissolution is evident in the study area and mainly occurred along the particle edges and cleavage (Figure 6e); later, the dissolution formed moulding porosity. Dissolution of the debris occurred after that of feldspar, and the minerals easily soluble in the debris were subjected to selective dissolution, which formed the intra-granular pores. Due to changes in water conditions, the early calcite cements were eroded and easily replaced by other minerals, partially clogging the pore space (Figure 7h). Microscopically, the plagioclase-sourced laumontite (Figure 7i) occupies some of the pore space. As the groundwater gradually became acidic, the laumontite began to dissolve along the cleavage plane, and the physical properties of the reservoir improved. The dissolution of feldspar and debris is usually caused by the uplift of tectonic movements and the charging of organic acids.

## 5. RESULTS ANALYSIS

### PARAGENETIC SEQUENCE OF THE DIAGENESIS

According to thin-section (400) and cathodoluminescence (122) observations, the space between particles is filled with clay (kaolinite and illite), and a small number of inter-granular pores are observed (Figure 6f). The observed chlorite film is closer to the particle surface than the calcite cement (Figure 6e), indicating that chlorite films formed earlier than the calcite cement [64]. The chlorite films disappear at the particle contacts, thus indicating that the chlorite film formed after the initial compaction. A small amount of calcite is observed on the syntaxial overgrowths (Figure 6b), indicating that the calcite formed after the syntaxial overgrowths. The diagenetic environment changed from alkaline to acid. The calcite also encompasses the residual kaolinite, suggesting that the calcite formed after the formation of argillaceous and siliceous cements. Authigenic quartz developed in the pores between the chlorite film (Figures 5b,6c), proving that the formation of the authigenic quartz occurred after the formation of the chlorite film.

Based on the abovementioned studies, the diagenetic sequence is as follows:

Mechanical compaction → Early stage of chlorite film precipitation → Authigenic quartz precipitation → Early stage of calcite precipitation → Illite and needle- and rosette-shaped chlorite precipitation → Feldspar dissolution → Kaolinite precipitation → Late calcite cementation

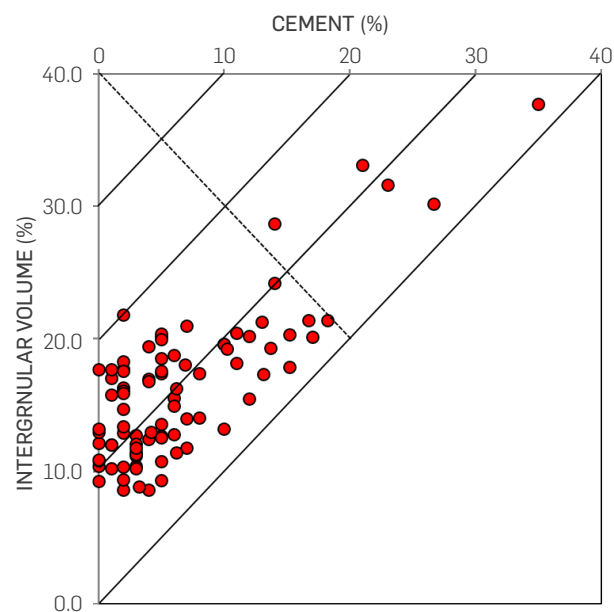


**Figure 7.** The relationship between intergranular volume (IGV) and cement volume in the Chang 8<sup>th</sup> reservoir.

### QUANTITATIVE EVALUATION

#### PRIMARY POROSITY

The original porosity was calculated by an empirical formula [65].

$$\Phi_0 = 20.91 + 22.9/S \quad (1)$$

where  $S$  refers to the sorting coefficient and  $\Phi_0$  refers to the original porosity. The original porosity of the Chang 8<sup>th</sup> reservoir is mainly between 30.1% and 41.7%, with an average value of approximately 34.3%.

#### POROSITY REDUCTION DUE TO COMPACTION

According to the quantitative statistics of the thin sections, the porosity after compaction can be calculated by the following formula.

$$\Phi_1 = \Delta V_{\text{cem}} + (S_{\text{pre}} + S_{\text{cem}}) * \Phi_{\text{now}} / S_0 \quad (2)$$

where  $\Phi_1$  refers to the porosity after the compaction,  $\Delta V_{\text{cem}}$  refers to cement content,  $S_{\text{pre}}$  refers to the plane porosity of the primary intergranular pores,  $S_{\text{cem}}$  refers to the plane porosity of cement,  $\Phi_{\text{now}}$  refers to the experimental porosity, and  $S_0$  refers to the total plane porosity.

$$\Phi_L = \Phi_0 - \Phi_1 \quad (3)$$

where  $\Phi_L$  refers to the porosity decrease due to compaction and  $\Phi_0$  refers to the primary porosity.

The reservoir porosity substantially reduced due to compaction; it decreased an average 24.8% from the original porosity (Figure 8).

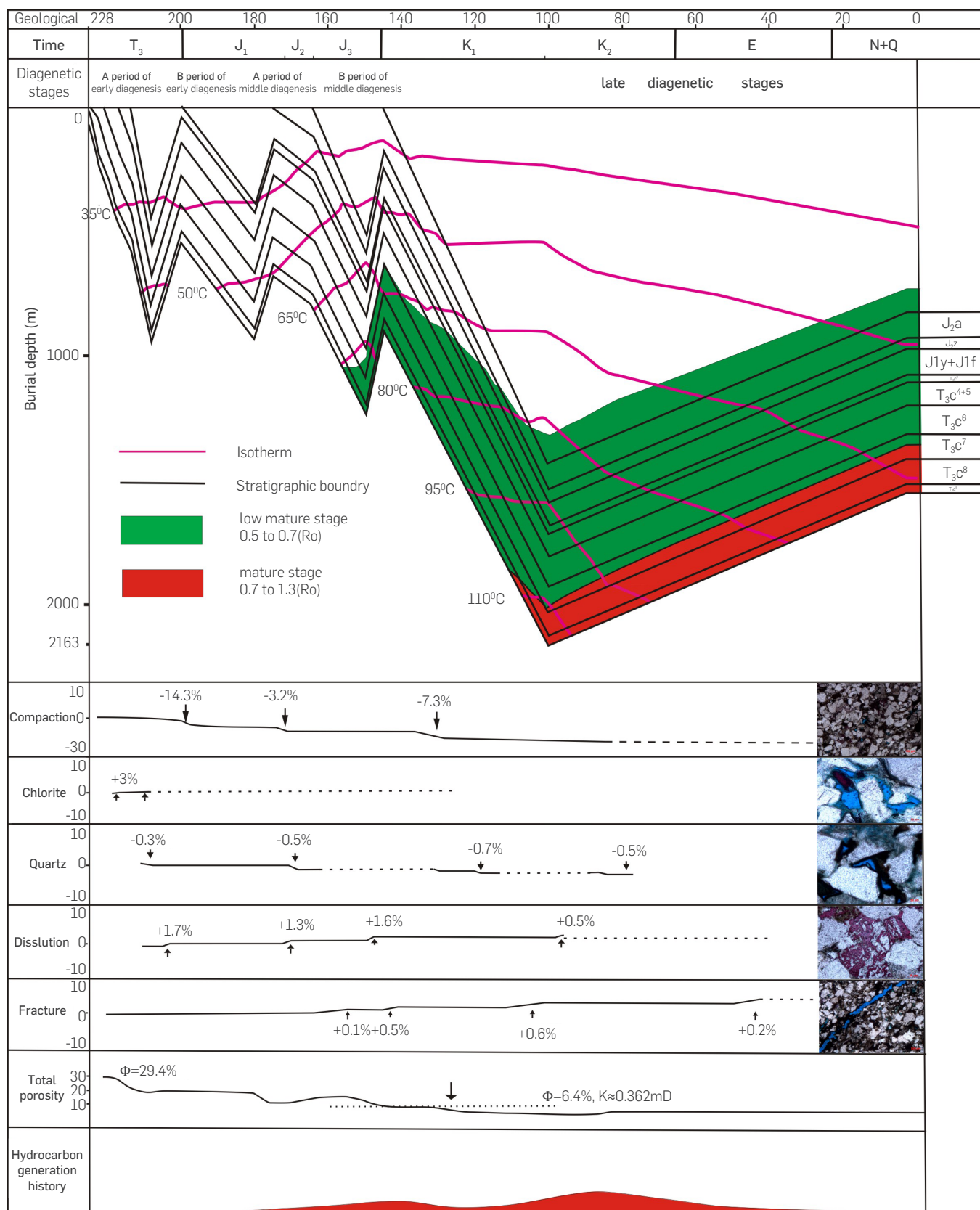


**Figure 8.** Thermal, burial, and diagenetic history and the porosity evolution of the Chang 8<sup>th</sup> sandstone reservoir in the Binchang area.

## POROSITY REDUCTION DUE TO CARBONATE CEMENTATION

$$\Phi_2 = (S_{\text{per}} / S_o) \times \Phi_{\text{now}} \quad (4)$$

$$\Phi_c = \Phi_1 - \Phi_2 \quad (5)$$

where  $\Phi_2$  refers to porosity after cementation and  $\Phi_c$  refers to the decrease in porosity due to carbonate cementation.

Carbonate cementation resulted in an average 8.2% decrease in the reservoir porosity.

## POROSITY REDUCTION DUE TO DISSOLUTION

$$\Phi_3 = (S_{\text{Intra}} + S_{\text{Inter}}) \times \Phi_{\text{now}} / S_o \quad (6)$$

where  $\Phi_3$  refers to the increase in porosity due to dissolution,  $S_{\text{Intra}}$  refers to the intra-granular dissolution from the plane porosity, and  $S_{\text{Inter}}$  refers to the inter-granular pore dissolution from the plane porosity.

The porosity increased by approximately 5.1 % due to dissolution (Figure 8).

## INFLUENCE OF OIL INVASION ON RESERVOIR

The porosity of reservoirs is positively correlated with oil saturation. The higher the oil saturation, the greater the porosity and permeability (Figure 4F). Four stages of large-scale oil invasion were taken in the study area. Early oil invasion is conducive to the protection of pores, which become the best space for the later large-scale oil invasion. The second time intervals of oil invasion in 122 Ma -110 Ma are large and last for a long time. Some reservoirs inhibit the diagenesis at this stage, which has significant influence on the pore evolution.

According to hydrocarbon inclusions data the homogenization of inclusions is mostly distributed in 70 °C-100 °C and 100 °C-130 °C.

Based on the historical analysis of reservoir formation in the study area (Figure 8), there are two stages of oil accumulation in the reservoir, which are 155 Ma -150 Ma and 140 Ma -120 Ma. Through the relationship between reservoir evolution and hydrocarbon charging, it can be concluded that during the early and middle stages of oil accumulation in reservoir, the reservoir is not densified; however, regarding oil accumulation in the late stage, the reservoir is in the densification stage.

## CONCLUSIONS

The Chang 8<sup>th</sup> sandstones are mostly feldspathic litharenites and lithic arkosic sandstones with low sandstone compositional maturity and relatively low textural maturity.

The Chang 8<sup>th</sup> reservoir properties are poor, with low porosity and permeability, small pore-throat radii, and high displacement and median pressures. Moreover, the physical properties are strongly heterogeneous, both laterally and vertically. The pore structures mainly consist of secondary dissolved pores and residual inter-granular pores.

Compaction, which reduced the reservoir porosity by 24.8%, and carbonate cementation, which reduced the reservoir porosity by 8.2%, are the main causes of densification in the Chang 8 reservoir. Compaction has played a more important role than cementation in decreasing the reservoir quality. Dissolution, which increased the reservoir porosity by 5.1 %, is the most important factor for increasing the reservoir porosity. In addition, chlorite plays an active role in inhibiting secondary quartz growth and preserving primary pores.

Two stages of oil accumulation in the reservoir can inhibit the diagenesis, which has a great effect on preserving primary pores.

## REFERENCES

- [1] Melo, R.C.B. and Lakani, R., 2012. Development of unconventional resources in North Africa: evaluation approach. SPE Paper 150406-MS. In: Presented at the North Africa Technical Conference and Exhibition, Cairo, Egypt, February 20–22, 2012.
- [2] Bhattacharya, S and Nikolaou, M, 2013. Analysis of production history for unconventional gas reservoirs with statistical methods. Society of petroleum engineers. 18 (5) :878-896.
- [3] Zou, C. N., Zhang, G. S., Yang, Z., Tao, S. Z., Hou, L. H., Zhu, R. K., Yuan, X. J., Ran, Q. Q., Li, D. H., Wang, Z. P., 2013. Concepts, characteristics, potential and technology of unconventional hydrocarbons: on unconventional petroleum geology. Petroleum Exploration and Development. 40, 385-399+454.
- [4] Cai, B., Ding, Y. H., Lu, Y. J., Shen, H., Yang, Z. Z., 2014. Status of unconventional oil and gas resources and its environment risk factors in China. Applied Mechanics & Materials. 541-542 :927-931.
- [5] Zou, C.N., Tao, S. Z., Bai, B., 2015. Differences and Relations between Unconventional and Conventional Oil and Gas. China Petroleum Exploration. 20(1), 1-16.
- [6] Zou, C. N., Zhu, R. K., Wu, S. T., 2012. Types, characteristics, genesis and prospects of conventional and unconventional hydrocarbon accumulations: taking tight oil and tight gas in China as an instance. Acta Petrolei Sinica. 33, 173-187.
- [7] Meissner, F. F., 1978. Petroleum geology of the Bakken formation Williston basin, North Dakota and Montana// Rehrig, D. Williston Basin Symposium: Billings, Montana. Montana Geological Society.
- [8] Miller, B.A., Paneitz, J.M., Mullen, M.J., Meijs, R., Tunstall, K.M., Garcia, M., 2008. The Successful Application of a Compartmental Completion Technique Used to Isolate Multiple Hydraulic-fracture Treatments in Horizontal Bakken Shale Wells in North Dakota. SPE Annual Technical Conference and Exhibition. Society of Petroleum Engineers.
- [9] Harbor, R.L., 2011. Facies characterization and stratigraphic architecture of organic-rich mudrocks, upper cretaceous Eagle Ford formation, South Texas. M.S. thesis. University of Texas at Austin. 184 pp.
- [10] Yu, X., Li, S., Yang, Z., 2015. Discussion on deposition-diagenesis genetic mechanism and hot issues of tight sandstone gas reservoir. Lithologic Reservoirs. 27, 1-13+131.
- [11] USGS, 2008. Assessment of undiscovered oil resources in the Devonian-Mississippian Bakken formation, Williston Basin Province, Montana and North Dakota. USGS Face sheet.
- [12] British Petroleum Company, 2011. BP statistical review of world energy: London, British Petroleum Company, 210 p.
- [13] Clarkson, C. R. and Pedersen, P. K., 2011. Production analysis of western Canadian unconventional light oil plays: Canadian Unconventional Resources Conference, November 15–17, Alberta, Canada, CSUG/SPE 149005, 22 p.
- [14] Vinchon, C., Giot, D., Sperber, O.F., Arbey, F., Thibieroz, J., Cros, P., Jeannette, D., Sizun, J. P., 1996. Changes in reservoir quality determined from the diagenetic evolution of Triassic and Lower Lias sedimentary successions (Balazuc borehole, Ard che, France). Marine and Petroleum Geology 13, 685–694.

- [15] Lai, J., Wang, G., Ran, Y., Zhou, Z., Cui, Y., 2016. Impact of diagenesis on the petrophysical properties of tight oil reservoirs: The case of Upper Triassic Yanchang Formation Chang 7 oil layers in Ordos Basin, China. *Journal of Petroleum Science and Engineering*, 145, 54-65.
- [16] Cao, Z., Liu, G. D., Zhan, H. B., Li, C. Z., Y. Y., Yang, C. Y., Jiang, H., 2016. Pore structure characterization of Chang-7 tight sandstone using MICP combined with N2GA techniques and its geological control factors. *Scientific Reports*, 6:36919.
- [17] Lai, J., Wang, G., Wang, S., Cao, J., Li, M., Pang, X., Zhou, Z., Fan, X., Dai, Q., Yang, L., He, Z., Qin, Z., 2018. Review of diagenetic facies in tight sandstones: Diagenesis, diagenetic minerals, and prediction via well logs. *Earth-Science Reviews*, 185, 234-258.
- [18] Cao, Z., Liu, G. D., Liu, Z. X. X., Yuan, Y. F., Wang, P., Niu, Z. C., Zhang, J. Y., 2014. Research status on tight oil and its prospects. *Natural Gas Geoscience*, 25(10): 1499-1508.
- [19] Bjørlykke, K., and Jahren, J., 2012. Open or closed geochemical systems during diagenesis in sedimentary basins: constraints on mass transfer during diagenesis and the prediction of porosity in sandstone and carbonate reservoirs. *AAPG Bulletin* 96, 2193-2214.
- [20] Zhang, S., Ding, X., 2010. Character sand causes of tight sand stones of Yanchang Formation in southern Ordos Basin, China. *Journal of Chengdu university of technology (Science & Technology Edition)*. 04, 386-394.
- [21] Zou, C.N., Zhu, R.K., Liu, K.Y., Su, L., Bai, B., Zhang, X.X., Yuan, X.J., Wang, J.H., 2012. Tight gas sandstone reservoirs in China: characteristics and recognition criteria. *J. Pet. Sci. Eng.* 88-89, 82-91.
- [22] Rahman, M.J.J. and McCann, T., 2012. Diagenetic history of the Surma Group sandstones (Miocene) in the Surma Basin, Bangladesh. *Journal of Asian Earth Sciences*. 45 (4), 65-78.
- [23] He, Z., 2003. Ordos Basin Evolution and oil and gas. Beijing: petroleum industry press. 91-104.
- [24] Ding, X., Zhang, S., Liu, Y., Liu, K., 2008. Distribution law of inner oil layer in sequence framework of Yanchang Formation in Jinghe area. 30 (2), 49-53+188.
- [25] Zeng, L., Li, X. Y., 2009. Fractures in sandstone reservoirs with ultra-low permeability: A case study of the Upper Triassic Yanchang Formation in the Ordos Basin, China. *AAPG Bulletin*. 93 (4), 461-477.
- [26] Sun, Z., Sun, Z., Lu, H., Yin, X., 2010. Characteristics of carbonate cements in sandstone reservoirs: A case from Yanchang Formation, middle and southern Ordos Basin, China. *Petroleum Exploration and Development*. 37(05), 543-551.
- [27] Ding, X. and Zhang, S., 2011. Diagenesis and its effects on physical properties of the southwestern margin of Ordos Basin in Mesozoic. *Petroleum Geology and Recovery Efficiency*. 18 (1), 18-22+112.
- [28] Dixon, S. A., Surdan, R. C., 1989. Diagenesis and preservation of porosity in Norphlet Formation (Upper Jurassic), southern Alabama. *Am. Assoc. Petrol. Geol. Bull.* 73: 707-728.
- [29] Li, S., Yao, J., Mou, W., Luo, A., Wang, Q., Deng, X., Chu, M., Li, Y., Yan, C., 2018. The dissolution characteristics of the Chang 8th tight reservoir and its quantitative influence on porosity in the Jiyuan area, Ordos Basin, China. *Journal of Natural Gas Geoscience*.
- [30] Zheng, L. J., Bao, H. P., Wu, Y. S., Sun, L. Y., Jiang, H. X., Ren, J. F., Huang, Z. L., Liu, L. J., 2018. Distinguishing coral reef facies from coral-bearing open platform facies: Examples from Ordovician Ordos Basin, Northwest China. *Palaeogeography, Palaeoclimatology, Palaeoecology*, 495:72-86.
- [31] Li, H., Wang, F., Dai, S., 2008. Influence of chlorite film on reservoir porosity: A case study from the second member of Yanchang Formation in Ordos Basin. *Lithologic Reservoirs*. 20 (4), 71-74.
- [32] Yang, H., Liu, Z., 2013. Provenance and depositional systems of the Upper Triassic Yanchang. *Earth Science Frontiers (China University of Geosciences (Beijing); Peking University)*. 20(2): 10-18.
- [33] Liu, X., 2014. Sandy clastic flow deposition and reservoir characteristics of Chang 8th formation in Binchang area, Ordos basin. *Reservoir Evaluation and Development*. 4(2), 2-8.
- [34] Zhang, Z., 2014. Binchang block south of Ordos Basin oil and gas accumulation Controlling factors and exploration direction. *Chemical Enterprise Management*. 2(2), 167-170.
- [35] Gao, S., Han, Q., Yang, H., Lin, F., Lin, H., 2000. Yanshanian movement in Ordos basin and its relationship with distribution of oil and gas. *Journal of Changchun University of Science and Technology*. 30 (4):35-358 (in Chinese).
- [36] Li, S. X., Deng, X. Q., Pang, J. L., Lv, J. W., Liu, X., 2010. Relationship between petroleum accumulation of Mesozoic and tectonic movement in Ordos Basin. *Acta Sedimentologica Sinica*, 28 (4): 798-807.
- [37] Yang, H., Liu, X., Zhang, C., 2007. The main controlling factors and distribution of low permeability lithologic reservoir of Triassic Yanchang Formation in Ordos Basin. *Lithologic Reservoirs*. 19(3), 1-6.
- [38] Chen, L. and Lu, Y., 2015. Sequence stratigraphy characteristics and filling evolution model of Yanchang Formation in southern Ordos basin. *Journal of Central South University (Science and Technology)*. 46(6), 2196-2206.
- [39] Yan, J., 2005. Sedimentary-tectonic evolution and gas-potential exploration of Late Paleozoic in Southern Ordos Basin. *Northwest University*. 1-162.
- [40] Yang, R., He, Z., Qiu, G., 2014. Late Triassic gravity flow depositional systems in the southern Ordos Basin. *Petroleum Exploration and Development*. 41(6), 661-670.
- [41] Yang, S., Wang, N., Li, M., 2013. The logging evaluation of source rock of Triassic Yanchang Formation in Chongxin area, Ordos Basin. *Natural Gas Geoscience* 24, 470-476.
- [42] Giles, M.R. and Boer, R.B.D., 1990. Origin and significance of redistributional secondary porosity. *Marine & Petroleum Geology*. 7 (4) :378-397.
- [43] Hu, F., Su, L., Wang, L., 2008. The Infection of Throat Radius and Percentage of Mobile Fluid for Leakage. *Inner Mongolia petrochemical industry*. 34 (24), 132-133.
- [44] Rezaee, R., Saeedi, A., Clennell, B., 2012. Tight gas sands permeability estimation from mercury injection capillary pressure and nuclear magnetic resonance data. *J. Pet. Sci. Eng.* 88-89, 92-99.
- [45] Lai, J., Wang, G., Ran, Y., Zhou, Z., 2015. Predictive distribution of high quality reservoirs of tight gas sandstones by linking diagenesis to depositional facies: Evidences from Xu-2 sandstones in Penglai area of central Sichuan basin, China. *Journal of Natural Gas Science and Engineering*, 23: 97-111.
- [46] Hayes, M.J. and J.R. Boles, 1992. Volumetric relations between dissolved plagioclase and kaolinite in sandstones: Implications for aluminum mass transfer in the San Joaquin Basin, California. In: *Origin, Diagenesis, and Petrophysics of Clay Minerals in Sandstones* (ED. By D. W. Houseknecht and E. D. Pittman), Spec. Publ. Soc. Econ. Paleont. Miner., 47:111-123.
- [47] Yu, B., Cui, Z., Liu, X., 2008. The Diagenesis of Chang-8 Reservoir Sandstone and Its Effect on Porosity in Xifeng Oilfield. *Journal of Jilin University*. 38(3), 405-416.
- [48] Marchand, A. M. E., Haszeldine, R. S., Smalley P. C., Macaulay, C. I., Fallick, A. E., 2001. Evidence for reduced quartz-cementation rates in oil filled sandstones. *Geology*, 29:915-918.
- [49] Bjørlykke, K., and J., Jahren, 2010. Sandstones and sandstone reservoirs. In: Bjørlykke, K. (Ed.), *Petroleum Geoscience: From Sedimentary Environments to Rock Physics*. Springer, Amsterdam, pp. 113-140.
- [50] Zhen, J., Zhao, S., Chen, C., 1988. Two different diagenetic Successions of Clastic Rock reservoir. *Geological Review*. 44(2), 207-212.
- [51] Anjos, S. M. C., DeRos L. F., Silva, C. M. A., 2003. Chlorite authigenesis and porosity preservation in the Upper Cretaceous marine sandstones of the Santos Basin, offshore eastern Brazil. *International Association of Sedimentology Special Publication*, 34(2):291-316.
- [52] Berger, A., Gier, S., Krois, P., 2009. Porosity-preserving chlorite cements in shallow-marine volcanoclastic sandstones: Evidence from Cretaceous sandstones of the Sawan gas field, Pakistan. *AAPG Bulletin*, 93(5):595-615.
- [53] April, R.H., 1981. Trioctahedral Smectite and Interstratified Chlorite/Smectite in Jurassic Strata of the Connecticut Valley. *Clays & Clay Minerals*, 29 (1) :31-39.
- [54] Wilkinson, M., Haszeldine, R. S., Milliken, K. L., 2003. Cross-formational flux of aluminum and potassium in Gulf Coast (USA) sediments. *MJ / Worden, R. H., Morad, S., Clay Mineral Cements in Sandstones. Special Publication of the International Association of Sedimentologists*. 34:147-160.
- [55] Mansurbeg, H., El-Ghali, M. A. K., Morad, S., Plink-Björklund, P., 2006. The impact of meteoric water on the diagenetic alterations in deep-water, marine siliciclastic turbidities. *Journal of Geochemical Exploration*. 89(1):254-258.
- [56] Wilkinson, M., Haszeldine, R.S., Fallick, A., 2006. Jurassic and Cretaceous clays of the northern and central North Sea hydrocarbon reservoirs reviewed. *Clay Minerals*. 41(1):151-186.
- [57] Tian, J., Gao, Y., Zhang, P., Wang, X., Yang, Y., 2013. Genesis of illite in Chang 7 tight oil reservoir in Heshui area, Ordos Basin. *Oil & Gas Geology*. 34 (5), 147-160.
- [58] Cao, Z., Liu, G. D., Kong, Y. H., Wang, C. Y., Niu, Z. C., Zhang, J. Y., Geng, C. B., Shan, X., Wei, Z. P., 2016. Lacustrine tight oil accumulation characteristics: Permian Lucaogou Formation in Jimusaer Sag, Junggar Basin. *International Journal of Coal Geology*, 153 :37-51.
- [59] Tang, H. F., Peng, S. M., Zhao, Y. C., Ai-Rong, L. I., 2007. Analysis of main control factors of the physical property of tight sandstone. *Journal of Xi'an Shiyou University (Natural Science Edition)*. 22(1):59-63.
- [60] Ge, Y., 2009. Effects of oil and gas charging on the growth of reservoir minerals - Evidence from synthetic hydrocarbon inclusions. 5th International Symposium on Hydrocarbon Accumulation Mechanism and Oil and Gas Resources Evaluation. 2009:7.
- [61] Ji, Y., Gao, C., Liu, Y., Lu, H., 2015. The impact of sedimentary characteristic on the diagenesis and reservoir quality of the 1st member of Paleogene Funing formation in the Gaoyousub basin. *Journal of Tongji University (Natural Science)*. 43 (1):133-139.
- [62] Worden, R.H., Oxtoby, N. H., Smalley, P. C., 1998. Can oil emplacement prevent quartz cementation in sandstones? *Petroleum Geoscience*. 4 (2), 129-137.
- [63] Xi, K. L., Cao, Y. C., Jahren, J., Zhu, R. K., Bjørlykke, K., Haile, B. G., Zheng, L. J., Helleberg, H., 2015. Diagenesis and reservoir quality of the Lower Cretaceous Qantou Formation tight sandstones in the southern Songliao Basin, China. *Sedimentary Geology*. 330, 90-107.
- [64] Liu, L., Huang, S., Wang, C., Huang, K., Tong, H., 2010. Cathodoluminescence Zonal Texture of Calcite Cement in Carbonate Rock and Its Relationship with Trace Element Composition: A Case of Ordovician Carbonate Rock of Tahe Oilfield, Tarim Basin. *Marine Origin Petroleum Geology*. 15(1), 55-60.
- [65] Weyl, P. K. and Beard, D. C., 1973. Influence of texture on porosity and permeability of unconsolidated sand. *AAPG Bulletin*, 57(2):349-369.